GEOPHYSICAL MAPPING OF LOST HISTORICAL SITES:

BRENHAM, TX

An Undergraduate Research Scholars Thesis

by

CHARLES EDWARD STANFORD

Submitted to Honors and Undergraduate Research
Texas A&M University
in partial fulfillment of the requirements for the designation as an

UNDERGRADUATE RESEARCH SCHOLAR

Approved by
Research Advisor: Dr. Mark E. Everett

May 2015

Major: Geophysics

TABLE OF CONTENTS

TABLE OF CONTENTS CONT.

Page

ABSTRACT

Geophysical Mapping of Lost Historic Sites: Brenham, TX. (May 2015)

Charles Edward Stanford
Department of Geology and Geophysics
Texas A&M University

Research Advisor: Dr. Mark E. Everett
Department of Geology and Geophysics

Brenham, Texas has an interesting past that may surprise some of its residents. This past is discoverable through the use of geophysical methods. The site in question is owned by Blue Bell Creameries and is located on South Chappell Hill Street. An old distillery is believed to have been built on this site and may be the first of its kind in Texas. To accurately identify the location of the historic building, multiple geophysical methods were used. The Magnetometer (MAG) measured any magnetic objects in the soil. Electromagnetic Induction (EMI) measured the apparent conductivity of the soil and sub-surface objects. Ground Penetrating Radar (GPR) recorded any relative dielectric permeability contrasts in the subsurface. Each of these techniques has drawbacks when used separately, but when combined these three methods provided a more complete picture of the sub-surface. MAG, EMI, and GPR all showed significant anomalies throughout the survey area. To combine the three methods, each technique's results were both qualitatively and quantitatively analyzed together. EMI and GPR were seen to correlate the best, showing significant sub-surface structures warranting further examination. Findings from future studies could be significant as the community's economy thrives on historical tourism.

ACKNOWLEDGEMENTS

I would like to thank Dr. Mark Everett for the opportunity and support he has provided throughout this project, also all those that helped collect data during the never ending Texas summer. And to my bros who were always ready to slash it; Tate Meehan, Tim de Smet, and Leo Keeler.

NOMENCLATURE

MAG	Magnetics
EMI	Electromagnetic Induction
GPR	Ground Penetrating Radar
s	Seconds
m	Meters – measurement of distance
cm	Centimeters – measurement of distance
m^2	Squared Meters – measurement of area
kHz	Kilohertz, 1000 hertz – measurement of frequency
MHz	Megahertz, 10^6 hertz
GHz	Gigahertz, 10^9 hertz
nT	nanoTeslas – the standardized unit for magnetic field
Tx	Transmitter
Rx	Receiver
HT	Hilbert Transform

CHAPTER I

INTRODUCTION

The historic town of Brenham, TX

Brenham, Texas is a small town in Washington County located in east central Texas. Brenham is home to many historical sites that are important in the history of Texas. It is important to continue to search for any pieces of Brenham's diverse past in order to have a complete historical picture of the town. Brenham's central location between Houston, Austin, and San Antonio makes it a major hotspot for historical tourism in the state. Because of this, any additional historical findings could be significant to the town's economy. The location of Brenham is shown in figure 1.

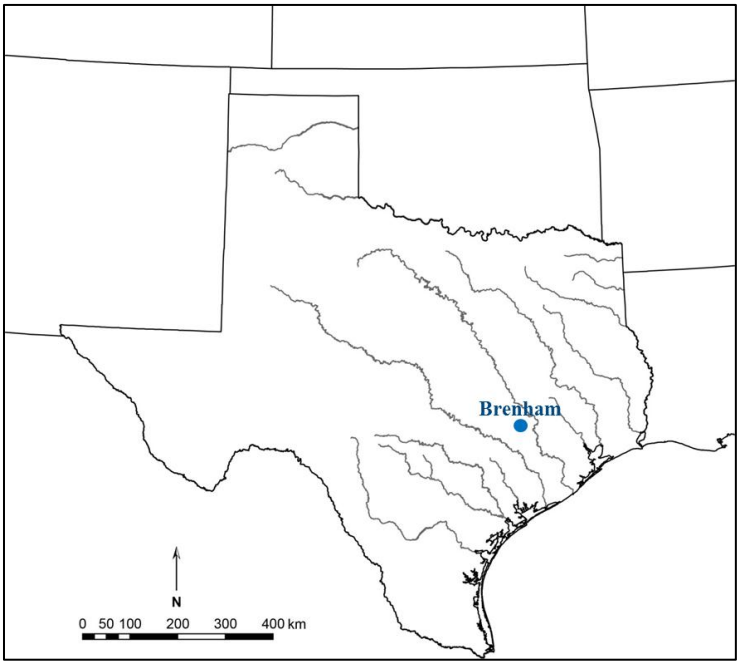

Figure 1 - Map depicting the location of Brenham and other significant Texas towns

Brief history of Brenham, TX

The town of Brenham was founded in 1844 when Texas was still a republic. The town was created by Washington County officials who needed a central hub to service a steep increase in population in the southwestern part of the county (Hasskal, 1933). Like many towns of the era, Brenham began as a small town with few residents and stores. Beginning in 1860 Brenham began operating a small railroad to Hempstead, TX. The railroad expansion was mainly financed by J.D. Giddings who organized the Washington Railroad Company with his brother. In 1871 the line was extended to Houston and Austin. The town experienced continuing expansion of rail lines up until 1905 when the current station was constructed. During this time the town experienced rapid economic growth associated with the railroads and quickly became "one of the most important little cities in the interior of Texas" (Hasskal, 1933 p. 8). In fact, during the Civil War, Washington County's population (15,500) exceeded that of Houston (9,000) and Austin (4,000) (Brass, 2011). It is during this time of rapid expansion that many buildings were built near the railroads and later abandoned as economic growth declined.

Property information

The geophysical study focuses on the property located at 507 South Chappell Hill St., Brenham, TX 77833. The Washington County Appraisal District identification number is R42537 shown in figure 2. The property is owned by Blue Bell Creameries, LP (W.C.A.D., 2014). The site has been utilized for several uses in the past decade, including a recreational baseball field in the north-west portion of the property near the intersection of S. Chappell and Seelhorse St. The property also has several small municipal water buildings near S. Chappell St. shown in figure 3. The main geophysical interest in the property is in the southern portion near a creek which acts

as one of the properties borders. In this area there is believed to be an old building, possibly one of the first distilleries in Texas. During a site investigation a visible mound was found in the suspected location.

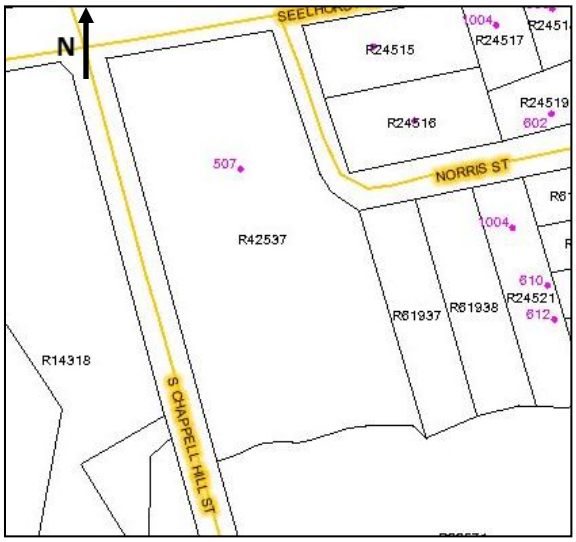

Figure 2 - Property map from Washington County appraisal district

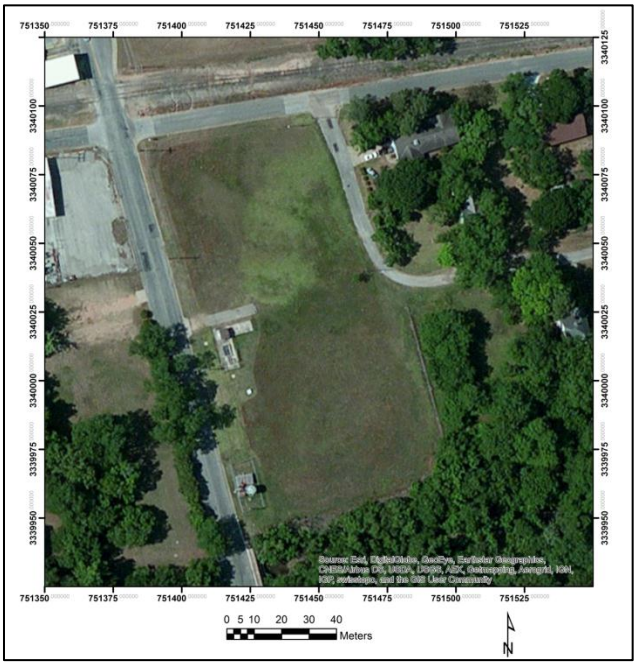

Figure 3 - Aerial property view from Google maps

Project objective

The ultimate objective of the project was to map the location of the unknown structure in the survey site. To confidently provide an accurate image of the subsurface, a variety of geophysical techniques were used. A secondary objective of the project was to increase the accessibility of geophysical equipment and software to students.

In order to accomplish these goals, geophysical techniques that measure different properties of the sub-surface were used. The Magnetometer measured any magnetic content in the soil. Electromagnetic Induction measured the apparent conductivity of the soil. Ground Penetrating Radar recorded any relative dielectric permeability contrasts in the subsurface. Each of these techniques has drawbacks when used separately, but when combined and correlated these three measurements provided a more complete picture of any objects present in the sub-surface.

Processing software and new survey equipment was also developed for this project in order to increase the accessibility of geophysical equipment for students. I hypothesized that combining the three geophysical techniques would yield a more accurate picture of the subsurface than using the techniques individually.

CHAPTER II

METHODS

The sub-surface mapping of the project location was completed using three geophysical techniques: Magnetics (MAG), Electromagnetic Induction (EMI), and Ground Penetrating Radar (GPR). The use of these three techniques increased the precision of the information about the sub-surface.

Survey grid construction

To tie all three geophysical techniques together, a common site grid was established. The grid location was chosen to be in the south area of the property near the area of interest found in a preliminary assessment of the site. Care was taken to keep the grid as far away as possible from the municipal water buildings located near Chappell Hill St shown in figures 4 and 5. These buildings have magnetic and electromagnetic properties that could have affected the survey results if care was not taken to minimize their effect. Other restrictions on the survey area were the sharply dipping creek bank on the southern border of the property, and a chain link fence on the eastern edge of the property.

Figure 4 - Municipal water building near Chappell Hill St.

Figure 5 - Municipal water building near Chappell Hill St.

Once the restrictions affecting the location survey grid were accounted for, the grid was constructed by using metric tape measures to define a Cartesian coordinate system as a 40 meter by 40 meter square. The origin point (0,0) of the grid was placed in the south-east corner, with the other corners (0,40), (40,0), and (40,40) being in the south-west, north-east, and north-west

respectively. To confirm that each corner was accurately placed in the square, the lengths of the diagonals were measured as 56.56 meters as calculated by the Pythagorean Theorem. This method was effective for creating the survey grid as the length of the diagonals was found to be within 5 cm of the correct lengths. This small error could be accounted for by the topography of the survey area and did not affect the results. Blaze orange non-magnetic surveyor spikes were used to permanently mark the corners of the grid so that in the future, geophysical surveys could be repeated in the exact same location. Figure 6 shows the grid location on an aerial photo with the coordinates of each corner marked. Figures 7, 8, and 9 depict the process of constructing the survey grid.

Figure 6 - Aerial of site with survey grid location in red

Figure 7 - Tate Meehan measuring the south-west corner of the grid

Figure 8 - Charles Stanford measuring the south-east grid corner

Figure 9 - Tim De Smet and Leo Keeler measuring the north-east grid corner

Data acquisition

All three geophysical techniques were collected in a similar manner. MAG and EMI surveys used .5 meter line spacing, traversing the Y-direction bi-directionally. Further defined, the data was collected on one line while moving in the positive Y-direction, once completed the line would then be moved .5 meters in the positive X-direction. Data would then be collected in the negative Y-direction with the process repeating until the survey is completed. An example can be seen in blue on figure 10. The GPR survey was collected with .25 meter line spacing uni-directionally, where each line began on the same side grid and traversed the same direction.

Continuous data collection was used due to several factors affecting geophysical surveys. In continuous data collection mode the equipment is set to acquire a data point once every set time interval. This method is much faster than discrete data collection, where data is collected only when prompted by the user. Because it is difficult to walk at a constant rate while collecting data continuously, fiducial lines were placed throughout the survey parallel to the x direction every 5 meters shown in green on figure 10. While collecting data, as a fiducial line was passed an

appropriate button was pushed to record a fiducial mark. It was then used during processing to better define the location of the data. While data collection in continuous mode is not as precise as discrete mode, continuous mode offers much greater speed without noticeably affecting the data quality.

Battery life of the equipment must also be taken into account. Because discrete surveys take much longer than continuous surveys, either extra batteries must be bought or more days in the field would be required to complete the full survey. Finally such a survey must account for sensor drift. Geophysical equipment has a tendency to "drift". Measurements in the same location readings will change throughout time due to outside factors. Therefore continuous mode was chosen in order to complete the geophysical surveys efficiently and to minimize the effects mentioned above.

Figure 10 – Bi-directional survey lines in blue and fiducial lines in green

Magnetics

Magnetometers are commonly used to measures the total intensity, |**B**| of the geomagnetic field. The geomagnetic field is very complex, with the primary contributor to the magnetic field being the rotation of iron bearing rocks within earth's outer core. However, many small scale features such as buildings, power lines, and geologic features also contribute to the geomagnetic field.

Magnetometers have many uses in geophysics today. They can be used to measure intrusive igneous rocks, weakly magnetized sedimentary rocks, faults, building foundations, pipelines, excavated areas, and anything that produces a change in the magnetic field (Everett 2013). The primary purpose of using the magnetometer in my survey was to detect any iron bearing artifacts associated with building structure. A simplified description of a magnetometer is shown in figure 11.

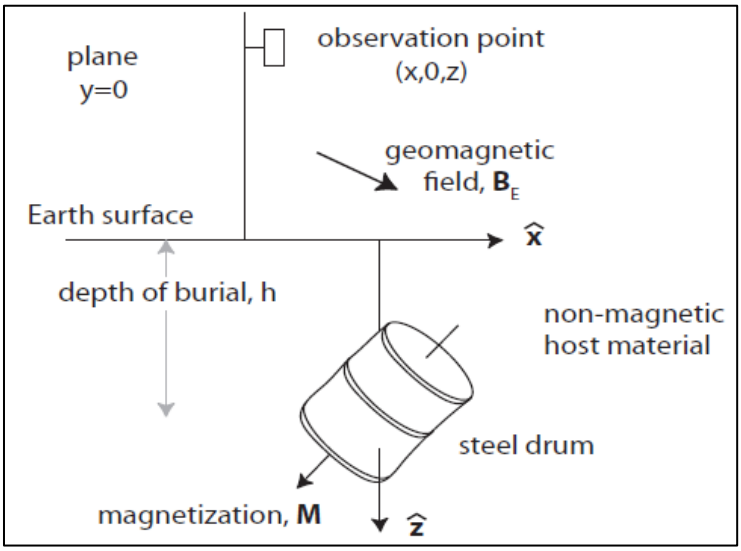

Figure 11 - Effect of objects on magnetometer readings from Everett 2013

Instrumentation

The G-858 Cesium Vapor Magnetometer was used in vertical gradiometer mode to complete the magnetics portion of the geophysical survey. The G-858 has several components; the logging console, an external 24 volt battery pack, and two magnetometer sensors. The logging console is powered by the external battery pack and is responsible for recording and storing of all data.

Typically measurements of the geomagnetic field range from 45,000 to 50,000 nanoTeslas (nT), the G-858 magnetometer is able to measure the magnetic field with a precision of 0.1 nT. Typical archeological magnetic anomalies can range from 100 to 1,000 nT. When used in gradiometer mode the G-858 calculates the difference in the measured |**B**| of two sensors. The spacing of these two sensors can be used to differentiate targets at different depths.

When used in vertical gradiometer mode, the two sensors of the G-858 are normally attached to an aluminum T staff directly above one another. While collecting data the console is attached to the users waist by a belt and the sensors are carried on the T-staff with the assistance of a shoulder strap shown in figure 12. There can be several sources of error associated with this method of data collection. It can be difficult to carry the sensors at a constant height and level throughout the survey. Because the sensors of the G-858 magnetometer are very precise, keeping the ground clearance height constant is very important in archeological applications.

Figure 12 - Typical set up of the G-858 Magnetometer in vertical gradiometer mode

Mag Cart

To reduce the effects of user error while operating the G-858 Magnetometer, a prototype Magnetometer Cart (Mag Cart) was designed and constructed shown in figure 13. The Mag Cart was designed to roll along the ground while keeping the sensors of the G-858 at a constant height of 0.4 and 0.9 meters. It was constructed out of ¾" PVC piping so that the cart did not have a magnetic signature. The wheels were made out of plastic and rubber for the same reason. Because the sensors would not attach directly to the ¾" PVC, the sensors were attached to the aluminum piping normally used. The aluminum piping was then connected to the PVC base. The Mag Cart was also designed with a handle with a simple bubble level attached. The level was used to make sure the sensors were perfectly vertical during operation.

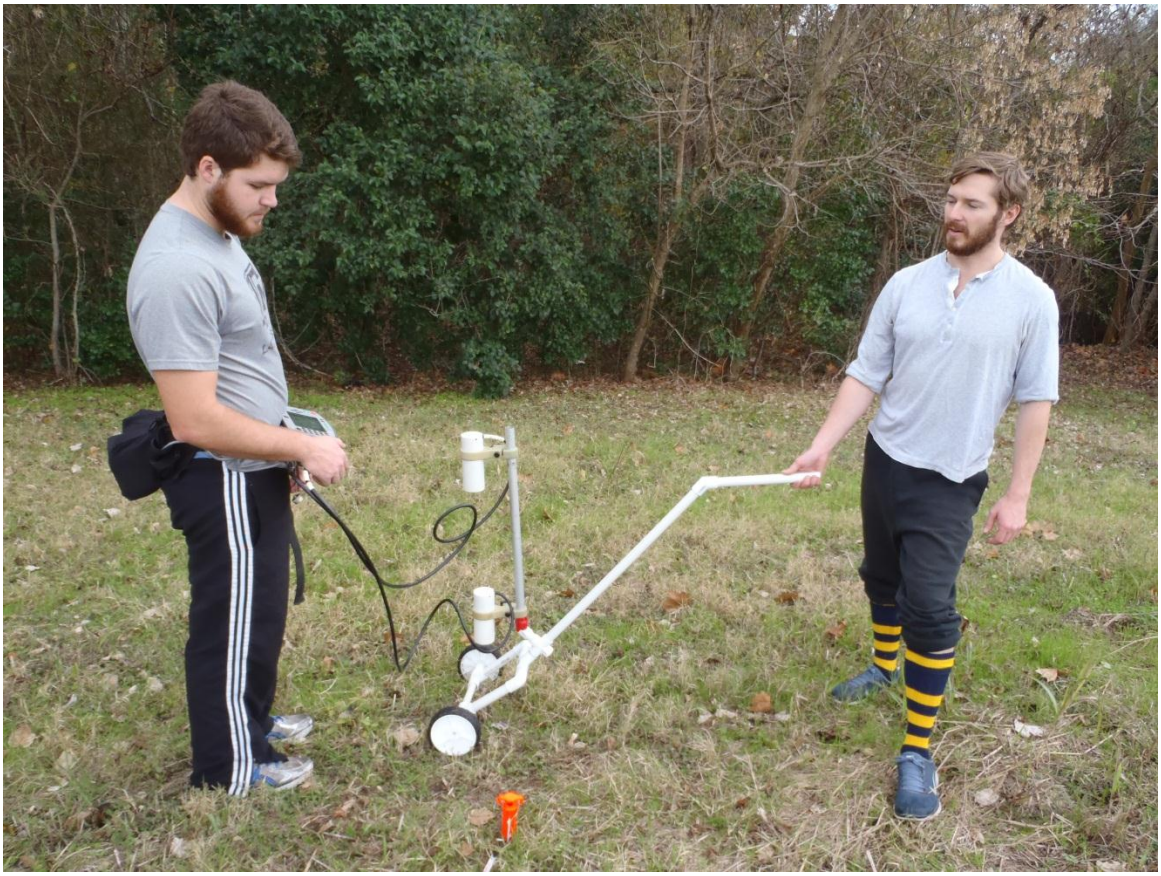

Figure 13 - Charles Stanford and Tim De Smet preparing to operate the Mag Cart

Acquisition

Before the survey began, all surveyors removed metallic items such as keys, belts, phones, wallets, and watches in order to reduce unwanted magnetic noise. The survey grid was then inspected for any surface material that could cause false anomalies. Metric tape measures were placed on all four sides of the survey grid. Fiducial lines were then placed every 5 meters parallel to the X-direction, and traversal lines were placed parallel to the Y-direction. To complete the magnetics survey, a team of five was used. Two people operated the Mag Cart and the G-858 logging console, two people operated the traversal line ropes, and one person was a designated note taker. Typically only one person will operate the G-858 logging console and hold the

sensors, but two people were chosen to operate the Mag Cart and Logging console so that each could focus solely on their task at hand. This method was effective at reducing human error normally associated with magnetometer surveys. Frequently when only one person operates the equipment they can lose track of either the sensor height or the operation of the logging console. The two people operating the traversal lines were in charge of moving several ropes separated 0.5 meters to indicate the line path that the magnetometer should be following. As the Mag Cart travelled over one line, the other lines would be lifted and moved to the position of next line to be traversed. This process allowed for greater speed while collecting the data. If only one line is used, the line must be completely travelled and then moved to the next position slowing data acquisition. The designated note taker was in charge of recording the position, direction travelled, and line number of each line collected as well as any mishaps and issues during the survey. This allowed for easier processing once the survey was completed.

Electromagnetic Induction

Maxwell's equations are the foundation of electromagnetic (EMI) geophysical methods. Inductive style geophysical equipment uses wire loop sources to avoid direct contact with the ground. Time-dependent current flows through the transmitter (TX) loop of wire inducing a primary EMI field. The receiver (RX) loop of wire then records the current produced by the present EMI field. In free space the system will record only the primary EMI field. If a conductive anomaly is present then the primary EMI field will flux through the anomaly and cause a secondary EMI field. The secondary field can then be picked up by the RX in addition to the primary EMI field. An example of this process is shown in figure 14. To record apparent conductivity of the target, the primary EMI field can be removed so that the secondary field is

isolated (Everett, 2013). EMI is able to measure changes in conductivity in the subsurface. Metallic objects give high or negative apparent conductivity, while objects such as bricks and foundations give low apparent conductivity measurements.

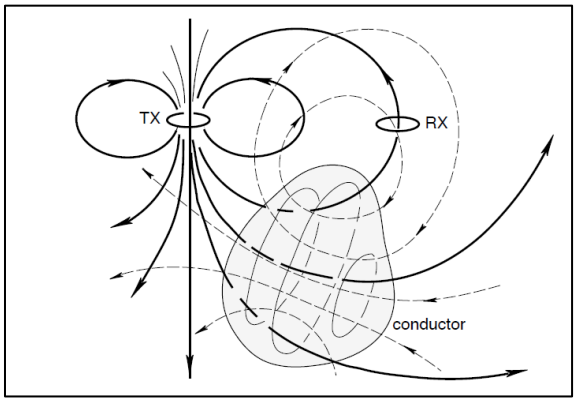

Figure 14 - Example of loop - loop Electromagnetic Induction from Everett 2013

Instrumentation

To complete the Electromagnetic Induction survey a GSSI Profiler EMP-400 was used. The EMP-400 profiler is a terrain conductivity meter with transmitter and receiver coils spaced 1.28 meters apart resembling a canoe paddle. A plastic handle was attached so that it may be carried 0.15 meters above the ground while surveying. During the survey, the Profiler was used in "spear" mode where the Profiler is parallel to the direction of travel. The EMP Profiler uses a handheld wireless data logger with integrated GPS and a real time data display. An example of the EMP-400 with data logger setup is shown in figure 15. The Profiler can collect data from three separate frequencies simultaneously, ranging from 1 kilohertz (kHz) to 16 kHz. Using three frequencies is beneficial because each frequency theoretically affects different depths in the subsurface. However, when using three frequencies the Profiler can only collect readings every 0.5 seconds. If only one frequency is used the Profiler can collect readings every .25 seconds.

Figure 15 - Charles Stanford demonstrating typical setup of the EMP-400 system

Acquisition

The EMI survey was collected in a similar manner to the magnetics survey. Surveyors removed all metallic and electronic items in order to reduce unwanted noise. Metric tape measures were again placed on all four sides of the survey grid. Fiducial lines were then placed every 5 meters parallel to the X-direction, and traversal lines were placed parallel to the Y-direction. To complete the magnetics survey a team of three was used. One person operated the EMP-400 Profiler, and two people operated the traversal lines. Since the profile is easier to use than the G-858 magnetometer only one person was required for operation. The transversal lines were operated the same as in the magnetics survey. No person was designated to take notes, as corrections could be made on the wireless data logger. The profiler was carried 0.15 meters above the ground, transmitted an 8 kHz signal, and sampled data every 0.25 seconds. Because the Profiler uses a slower sampling rate than the G-858, a slower walking speed was used while collecting in order to insure similar data spacing.

Ground Penetrating Radar

GPR and seismic geophysical methods both image the subsurface by measuring the travel times of transmitted and received signals. Seismic uses energy waves caused by concussive sources like explosions or hammer strikes, while GPR transmits electromagnetic waves. The electromagnetic waves are transmitted and received by closely spaced antennas. GPR sends out electromagnetic wave pulses that travel through the ground and reflect at any interfaces or artifacts in the subsurface. Typically GPR equipment has a frequency range of 10 megahertz (MHz) to 1 gigahetrz (GHz) whereas seismic typically has frequencies that are much lower (Everett 2013). Because GPR has much higher frequencies than seismic it also has much better resolution.

Once a signal is transmitted, then any reflected waves travel back to the GPR receiver. The travel time and amplitude of the wave is recorded as a single GPR trace. A single GPR trace is equivalent to a single reading for the Magnetometer or the EMP Profiler. Each trace uses the two-way travel time since it must travel down and then reflect back up to the receiver. The two-way travel time is used to determine the distance to the cause of reflection using the velocity of the EMI wave.

The condition of the survey area is important when selecting the appropriate GPR equipment. EMI waves tend to attenuate or lose signal strength when traveling through a media. The primary factors affecting attenuation are the water and clay content of the subsurface. High water and clay content will cause the image quality to decrease. Low frequency waves have longer wavelength and can be used to image deeper than high frequency waves in poor soil conditions.

Unfortunately, using a low frequency also causes the vertical resolution to decrease (Everett, 2013). If the survey area is affected by clay and high water content, low frequency antennae should be used. If the site is not affected by high water and clay content, high frequency antennae will give the best image resolution.

Instrumentation

To complete the GPR survey the Sensors and Software PulseEkko Pro GPR system was used with 500 MHz antennae. This system has the ability to resolve objects up to 1.5 meters of depth. The antennae are housed in a flat-bottomed shielded sled that protects from noise and allows the antennae to be moved easily when pulled by the T-shaped handle. An odometer, consisting of a wheel that measures rotation as the sled is moved, was attached to the sled. The odometer helps define the location of the sled along the transversal line while collecting data. The antennae and odometer are controlled by a portable computer attached to the surveyor by a harness. The computer controls all aspect of the GPR survey and reads out data in real time on a digital display. Typical setup of the PulseEkko is shown in figure 16.

Figure 16 – Charles Stanford demonstrating typical setup of the PulseEkko system

Acquisition

The GPR survey was conducted similarly to both the EMI and Mag surveys. The only difference was that the GPR survey was conducted in a uni-directional manner. Each line began on the same side of the grid and travelled in the same direction each time. Surveyors removed all metallic and electronic items in order to reduce unwanted noise. Metric tape measures were again placed on all four sides of the survey grid. .25 meter line spacing and trace spacing of 2 cm was used to increase the resolution of the GPR survey. Fiducial lines were then placed every 5 meters parallel to the X-direction, and traversal lines were placed parallel to the Y-direction. To complete the magnetics survey a team of three was used. One person operated the PluseEkko system, and two people operated the traversal lines. Two sub-grids were chosen to acquire the GPR survey over. These sub-grids were in areas on high anomaly areas shown in the MAG and EMI surveys.

CHAPTER III

DATA PROCESSING

Once the data from the three geophysical techniques was collected, the data was processed with a combination of proprietary and commercial software packages in order to achieve optimal results.

GeopMapper

GeopMapper is a software package created in MATLAB to process MAG and EMI data for this project. MATLAB was chosen for the processing software because many students already have experience in MATLAB through required classes. This removes the necessity to learn a new programing language to be able to process geophysical data. The program processes text files exported from MagMap2000 and applies several processing functions to the data. GeopMapper has the following functions: De-Spike, Interpolation, Line Correction, Smoothing, Gradient Calculation, and Surfer Export.

De-spike

Geophysical data occasionally has “spikes” or readings that are not consistent with readings in the rest of the survey. Spikes can be much higher or much lower than the rest of the survey and only appear for one reading; therefore they can be determined to be caused by sensor issues. The De-spike function in GeopMapper uses a user determined de-spike height to search for spikes in the data. Any reading that jumps higher than the de-spike height from the previous and next reading is removed and the average value of the previous and next reading is inserted in its place.

Line 10 of the MAG data with a spike is shown in figure 17; in figure 18 the spike has been removed.

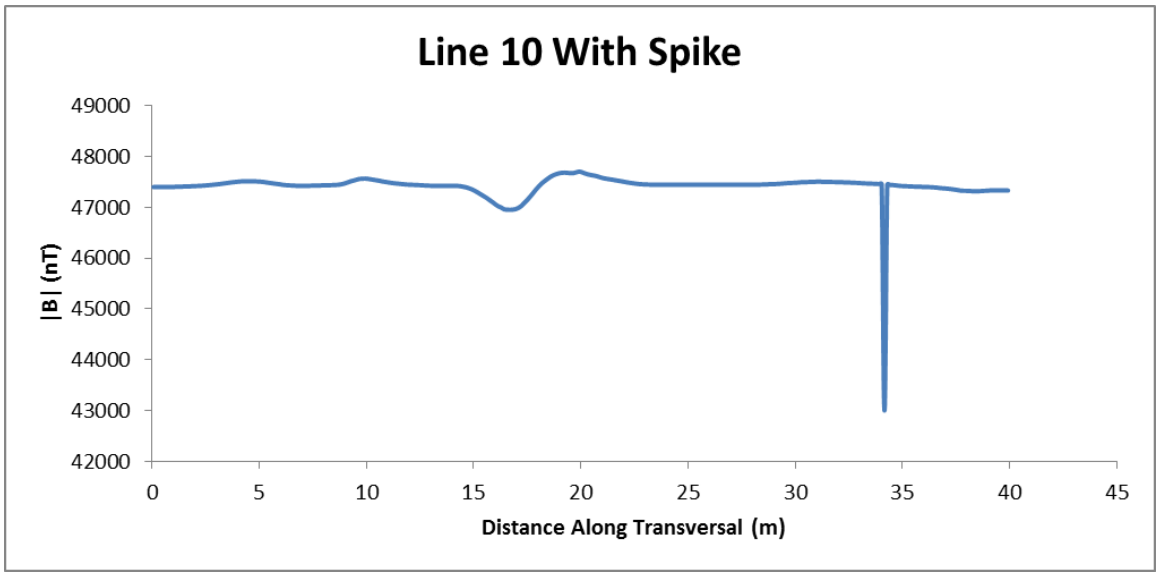

Figure 17 - Line 10 MAG data with spike

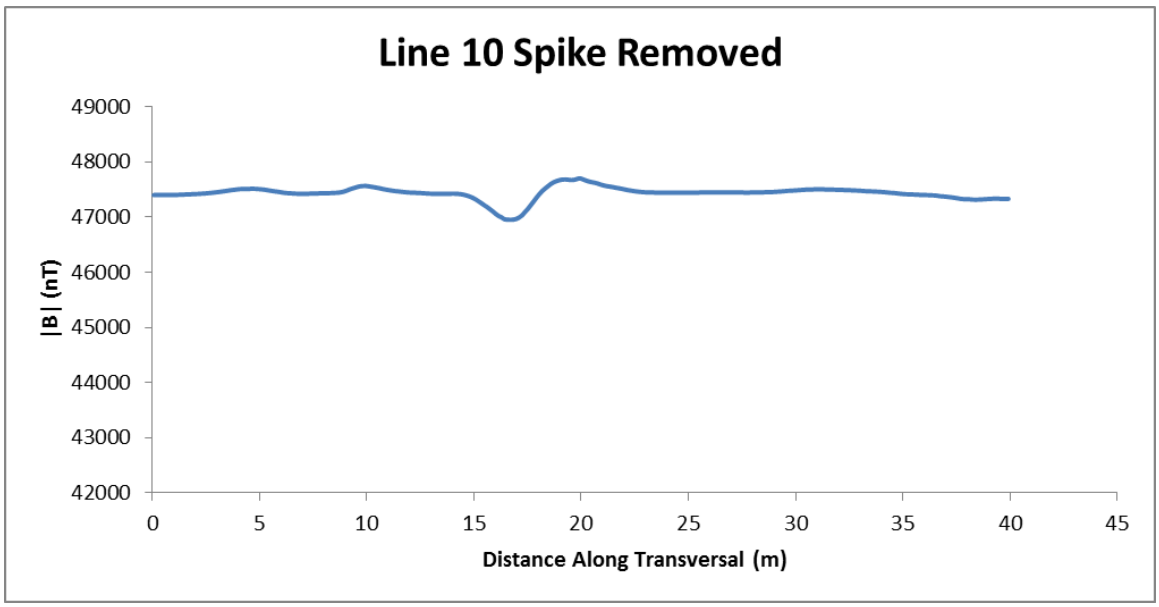

Figure 18 - Line 10 MAG data with spike removed

Interpolation

The GeopMapper Interpolation function uses Matlab's built in meshgrid and griddata functions to interpolate the geophysical data on to an evenly spaced grid with size and point spacing defined by the user. The biharmonic spline method was chosen for interpolation to provide the smoothest results. Both MAG and EMI data were collected at 0.5 meter line spacing. An even grid 40 x 40 meters in size with 0.25 meters point spacing was chosen to best represent the MAG and EMI data. This created an even grid 161 by 161 data points.

Line Correction

Geophysical data is sometimes affected by outside environmental factors. Telephone wires, electric cables, and radio waves can all have an effect on geophysical readings. This is commonly seen as striping of data sets, or lines traversing certain directions having overall higher readings than lines traversing other directions. EMI data can also be affected by temperature changes while collecting. Both of these problems can be solved by using GeopMapper's Line Correction function. The Line Correction function takes the median data value of each traversal line and compares it to the median data value of Line 0. If the median value of a traversal line was higher than that of line 0, all values in the traversal line have that difference subtracted, or added if the median was lower than that of line 0. The mean value of each line also can also be used, but is more sensitive to outliers causing it to be less effective when anomalies are present.

Smoothing

Smoothing was used to improve the appearance of the geophysical data. GeopMapper's smoothing function is a common weighted grid smoothing filter. A smoothed data point was calculated from the weighted average of a 3x3 point window around the original data point. The center point, the adjacent points, and the diagonal points can each have different weights or importance in the average. Figure 19 shows a representation of GeopMapper's Smoothing function. Data points are represented by individual squares. The squares on the left of figure 19 represent the 3x3 window of data points that the function uses. A, B, and C are the weights of the center, adjacent, and corner points respectively. The square on the right represents the single data point that is calculated by the function.

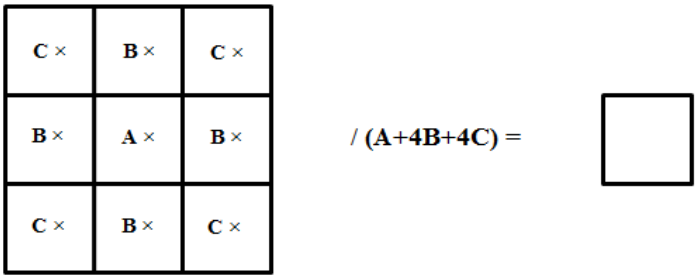

Figure 19 - Representation of GeopMapper Smoothing Function

Gradient Calculation

GeopMapper's Gradient function calculates the magnetic gradient of a two sensor magnetometer. The gradient equation is shown in equation 1.

$$Gradient = \frac{|B|_1 - |B|_2}{\Delta} \quad (1)$$

Where $|B|_1$ is the magnetic field strength of sensor 1, $|B|_2$ is the magnetic field strength of sensor 2, and Δ is the sensor spacing in meters.

Export

Once GeopMapper has completed all filtering operations, the data can be exported to surfer grid and column text files to allow for further processing.

Magnetics

Processing MAG data began with uploading the data from the G-858 Magnetometer logging console using MagMap2000 software by Geometrics. Using MagMap2000, survey information such as starting location, line spacing, fiducial spacing, and traversal direction can be applied to the raw data. Any mistakes during data acquisition were also corrected at this time. MagMap2000 then exported the data into several common file formats.

Diurnal correction

The data was diurnally corrected to account for temporal variations. Temporal variations can be caused by solar activity in the regional as well as several other factors. Multiple transversals of "Line 0" throughout the survey period were used to account for any temporal variation. The diurnal correction can be treated as a linear correction over short time periods. Equation 2 shows the application of the drift correction where $|B|_{dc}$ is the drift corrected magnetic field strength, $|B|$ is the observed magnetic field strength, m_{dc} is the slope of the drift correction and Δt is the time since the start of the survey for the reading.

$$|B|_{dc} = |B| - m_{dc} \times \Delta t \quad (2)$$

Both $|B|$ and Δt are values logged by the G-858 magnetometer. Multiple passes over "Line 0" were used to find m_{dc} using equation 3.

$$m_{dc} = \frac{\Delta|B|}{\Delta t} \quad (3)$$

Where Δ|B| refers to the change in field strength and Δt refers to the change in time between the two lines over line 0. Once the diurnal correction was completed, theoretically any reading taken over the same spot should have the same value of |B| each time in the absence of any other outside factors. An example of sensor drift over Line 0 is shown in figure 20.

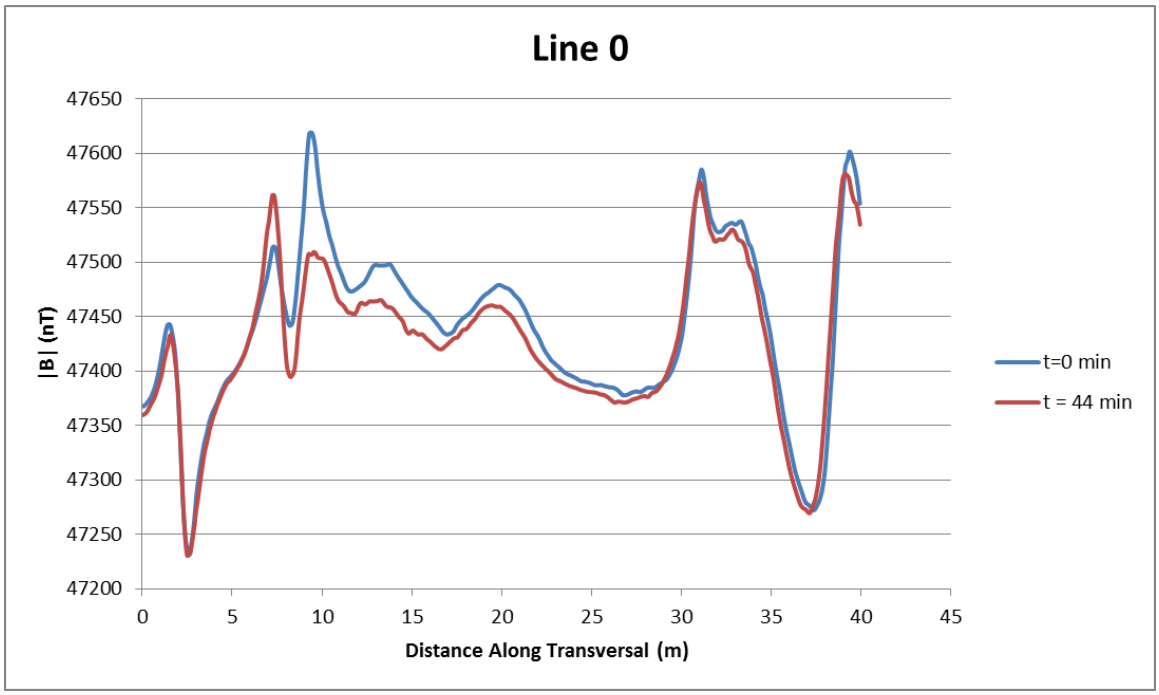

Figure 20 - Line 0 MAG drift example

GeopMapper

The diurnally corrected MAG data was uploaded to GeopMapper as a text file. The Mag data was processed using the De-Spike, Interpolation, Line Correction, Smoothing, Gradient Calculation, and Surfer Export functions. The exported files were contoured in Surfer by Golden Software. Figures 21, 22, and 23 show the top sensor, bottom sensor, and the magnetic gradient respectively.

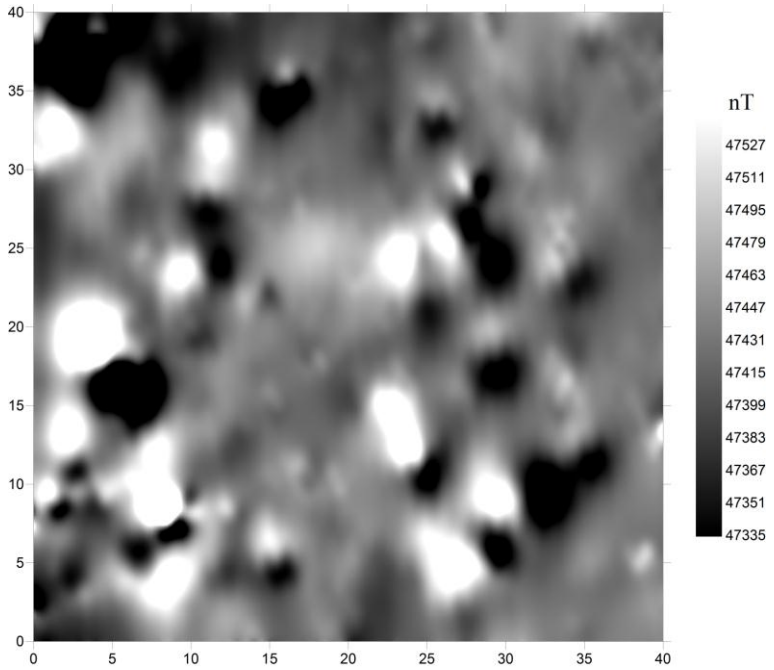

Figure 21- Magnetics Results (Top Sensor)

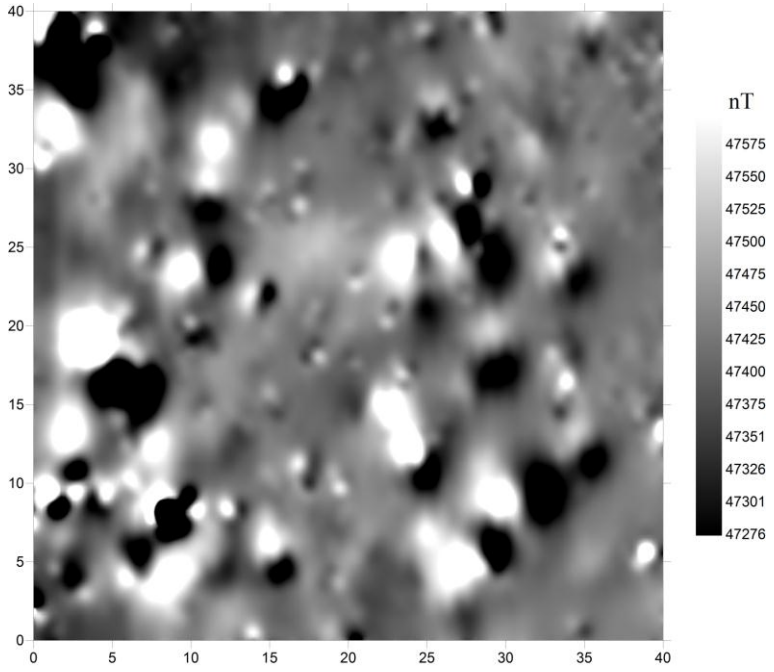

Figure 22 - Magnetics Results (Bottom Sensor)

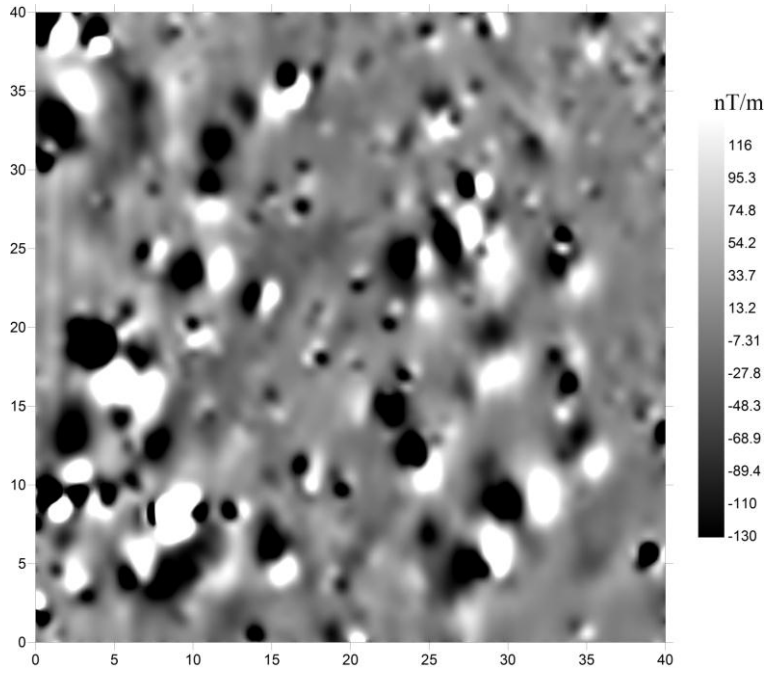

Figure 23 - Magnetics Results (Vertical Gradient)

Electromagnetic Induction

EMI data is processed in a similar manner to MAG data. Processing begins with uploading the data from the EMP-400 logging console using MagMap2000 software by Geometrics. Using MagMap2000, survey information such as starting location, line spacing, fiducial spacing, and traversal direction can be applied to the raw data. Any mistakes during data acquisition were also corrected at this time. MagMap2000 then exported the data into several common file formats.

GeopMapper

The EMI data was uploaded to GeopMapper as a text file. The EMI data was processed using the Interpolation, Line Correction, Smoothing, and Surfer Export functions. The exported file was contoured in Surfer by Golden Software. Figure 24 shows the conductivity of the 8 kHz survey, and figure 25 shows the In-Phase component of the magnetic field.

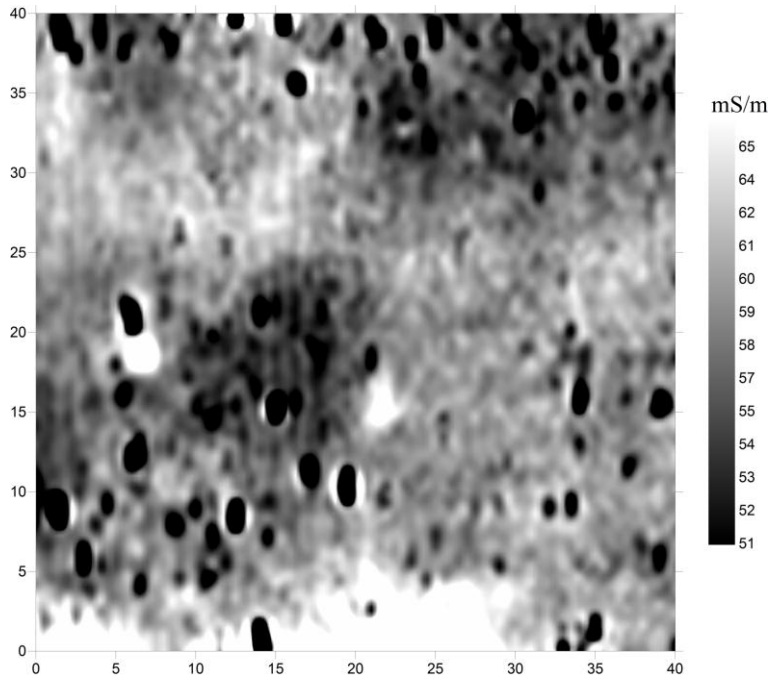

Figure 24 – EMI Conductivity (8kHz)

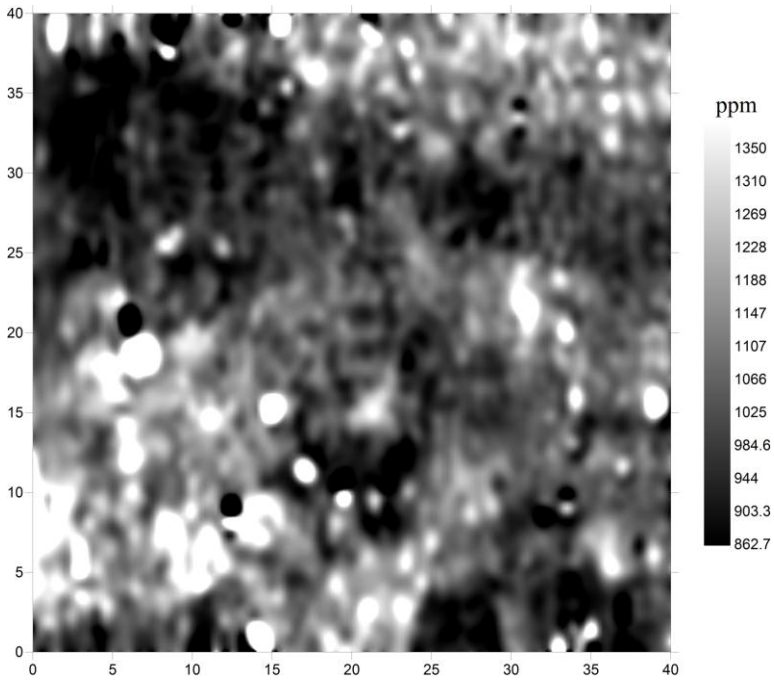

Figure 25 – EMI In-Phase Component (8 kHz)

Ground Penetrating Radar

The GPR survey was completed over two sub-grids of the larger main grid. Sub-grid A, the 20 by 20 meter grid in the lower portion of the survey seen in figure 26 below, was chosen due the high anomaly density seen in the MAG and EMI results. Sub-grid B, the 5 by 5 meter seen in the upper portion of the main grid was chosen because a strongly correlated anomaly was seen in the MAG and EMI surveys. Sub-grid B was used primarily to examine the benefits of the Hilbert Transform in regards to the correlation of MAG and EMI data. Line spacing of .25 meters and trace spacing of .02 meters was used. Once the GPR data was collected it was processed using EKKO-Mapper by Sensors and Software. In most processing steps the traces were processed individually.

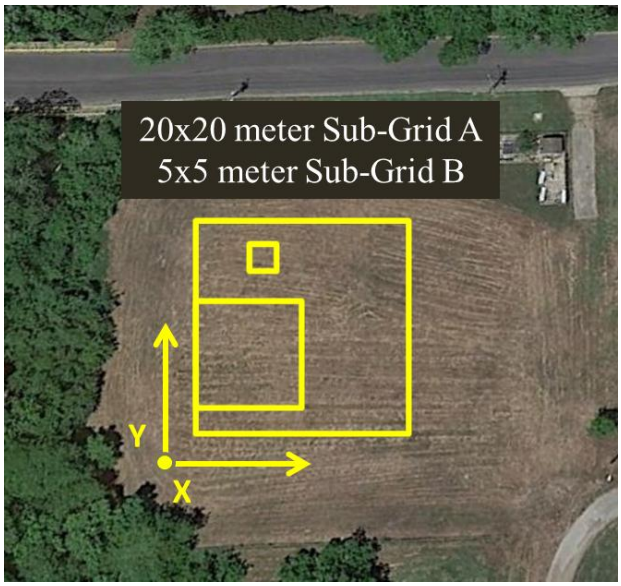

Figure 26 - Location of GPR Sub-grids

De-Wow

There were several steps to process the data. Each trace must first be De-Wowed. Wow is the shift in baseline amplitude of the GPR trace throughout time (Everett 2013). Typically this is treated in a linear fashion and an example of the filter can be seen in figure 27.

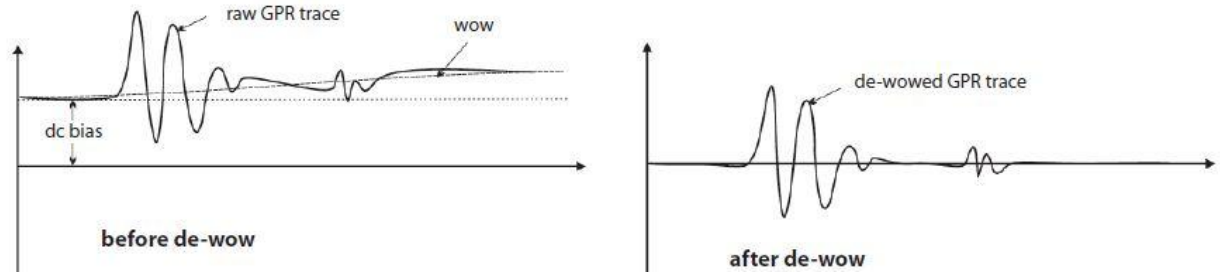

Figure 27 - De-Wow filter example from Everett 2013

Band-Pass Frequency Filtering

GPR systems are labeled by their central frequency, but actually operate on a broadband spectrum. Typically the frequency ranges from half of the central frequency to double the central frequency. As a 500 MHz system was used, the transmitted frequency could range from 250 MHz to 1000 MHz. Many electronics also operate in these frequency ranges and can therefore contribute to noise recorded by the RX. To reduce the noise from unwanted sources, the trace data can be band-pass filtered. The trace data is first transformed into the Fourier frequency domain where unwanted frequencies are removed. The trace data is then transformed back into the time domain by the inverse Fourier transform resulting in a trace with only the wanted frequencies. An example of a band-pass filter in frequency domain is shown in figure 28. In the example, amplitudes below frequency 1 (f_1) and above frequency 2 (f_2) will be removed.

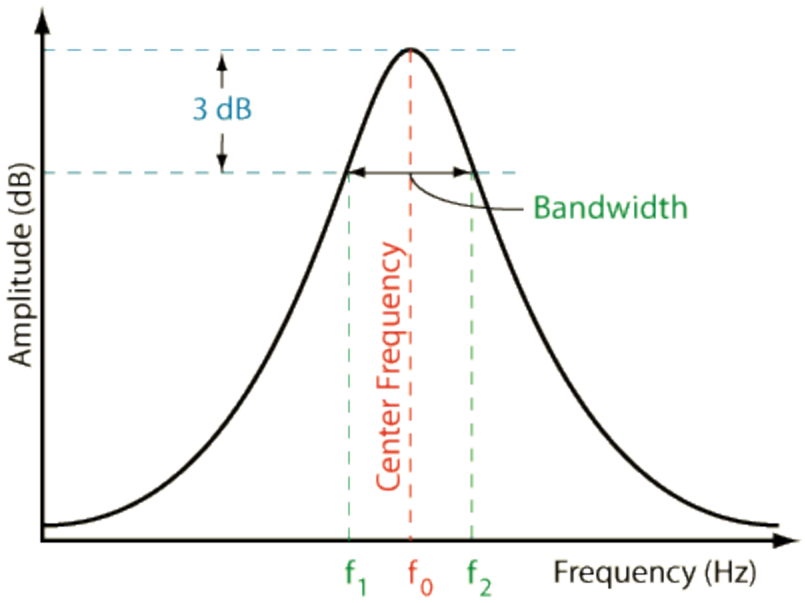

Figure 28 - Example of a Band-Pass Filter

Gain Control

As discussed before, EMI waves attenuate as they travel through a medium. This results in different reflection amplitudes at different depths even if the feature causing the reflection is the same. To remove this effect each GPR trace can be gain controlled, or amplitudes at greater depths can be increased. Figure 29 shows an example of an Automatic Gain Control (AGC) function. The AGC works by multiplying the inverse signal strength of the raw trace (Everett 2013). For the GPR survey a Spherical and Exponential Compensation (SEC) Function was used to gain control the data. A SEC gain was chosen over an AGC gain in order to preserve weak reflectors.

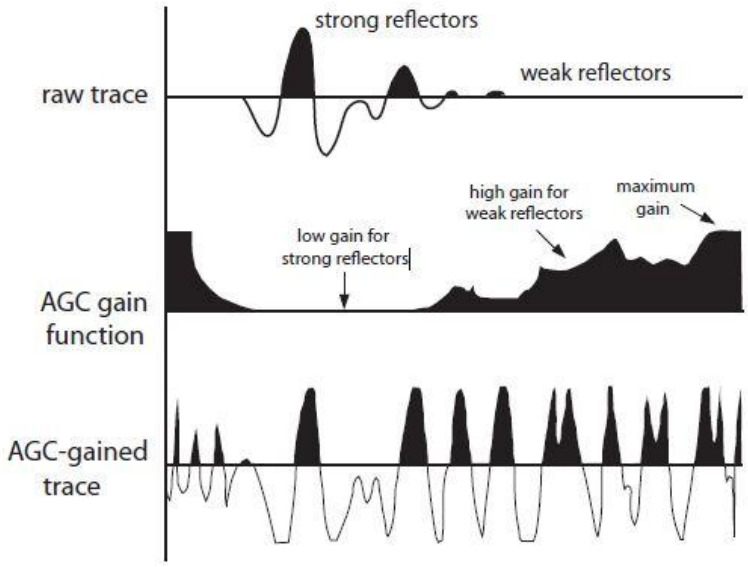

Figure 29 - Example of AGC Gain from Everett 2013

Background Removal Filter

A background removal filter removes signals caused by ground clutter and TX-RX cross-talk seen in the early portion of GPR traces. With the background noise removed, near-surface objects can be better imaged.

Migration

GPR trace data is collected in the time domain and must be converted to depth values by migration. This step is essential to GPR surveys used for archeological purposes as it gives the depth to the desired object instead of time. Migration is accomplished by finding the EMI wave velocity in the background medium, and converting the time values to depth values. In the survey area the background EMI wave velocity was found to be .077 meters per nanosecond (m/nS).

Instantaneous Amplitude Depth Slices

Once all of the above processing steps have been completed the traces were combined into depth slices. The depth slices depict the instantaneous amplitude at a specific location and depth, which is useful for depicting the location of objects causing reflections at different depths. The instantaneous amplitude is found by examining the analytic signal of each GPR trace using the Hilbert Transform. The Hilbert Transform essentially converts negative amplitudes into positive amplitudes and will be discussed in depth below. The resulting depth slice from 5 to 10 cm depth is shown below in figure 30.

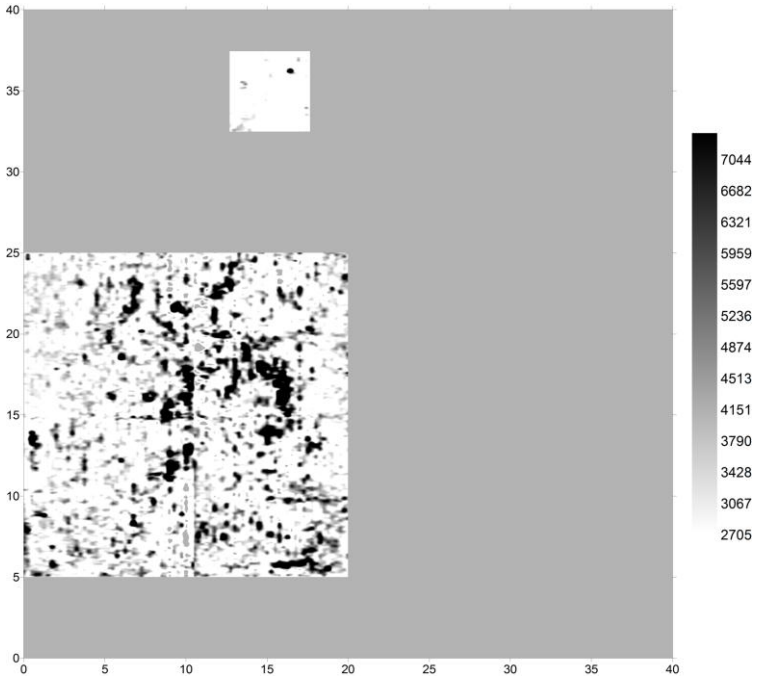

Figure 30 - GPR depth slice (5-10cm)

Hilbert Transform

The Hilbert Transform (HT) is commonly used in complex trace analysis of seismic and GPR data. The HT uses the real trace to compute the quadrature or imaginary trace. From the

quadrature trace, several diagnostic values can be calculated (Tanner 1979). An example of the quadrature trace is shown below in figure 31. The HT can also be used for different types of geophysical data. The absolute value of the HT was used in order to represent MAG and EMI anomalies. The absolute value of the HT is shown in figure 32 below.

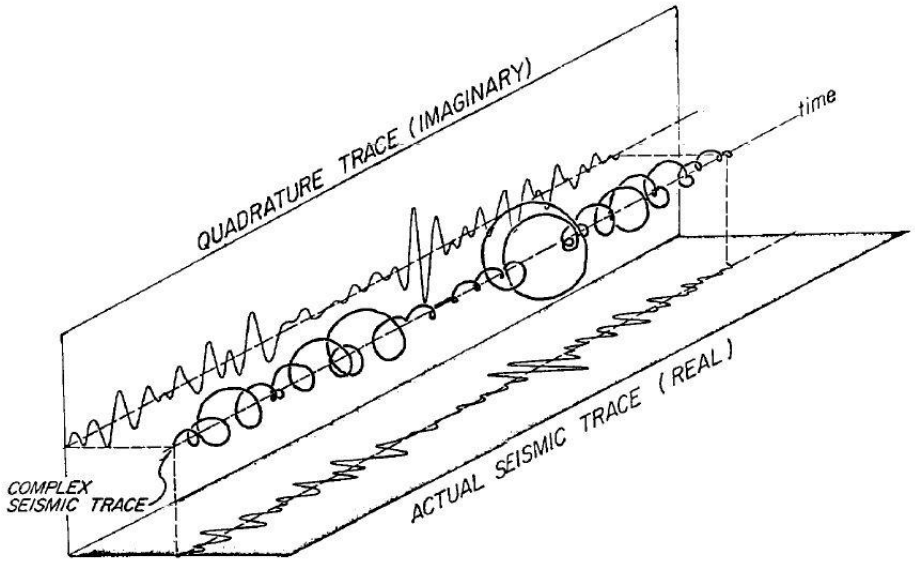

Figure 31 - Example of the Complex Trace from Tanner 1979

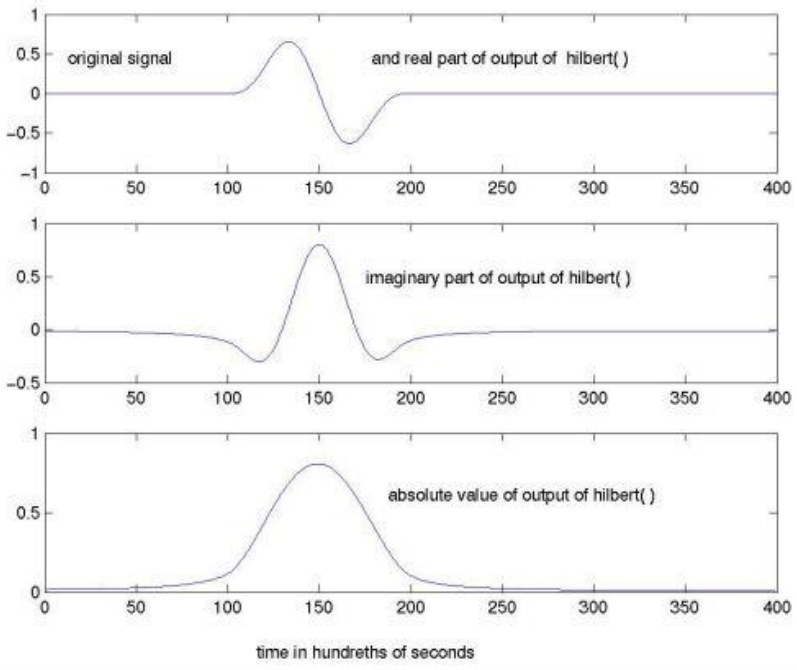

Figure 32 - Example of the Absolute value of the Hilbert Transform from Young 2004

MAG vs. EMI

The nature of MAG and EMI anomalies are inherently different. MAG anomalies are typically represented by an increase then decrease in magnetic field magnitude referred to as a dipole. EMI anomalies typically exhibit only a decrease or only an increase in magnitude referred to as positive or negative monopoles. In figure 33 below a MAG (blue) and EMI (red) transect over the anomaly found in sub-grid B is shown. Even though qualitatively it can be seen that the MAG dipole and EMI monopole are in similar locations, quantitatively it is hard to determine that they are in similar locations. The HT created all positive monopoles that are more quantitatively able to be correlated.

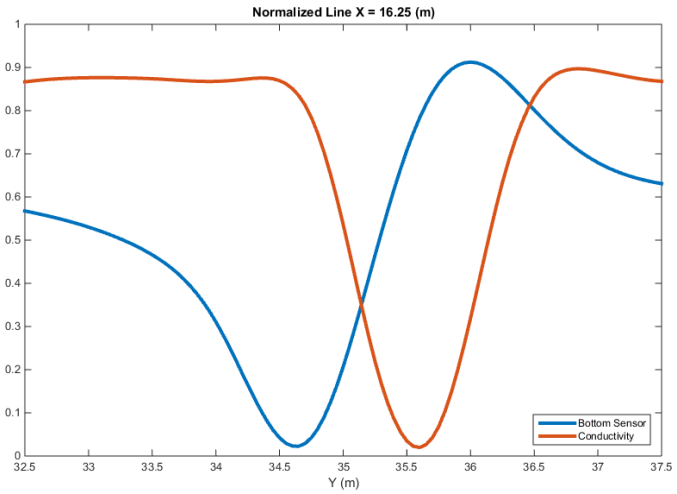

Figure 33 - MAG and EMI transect in Sub-grid B

Figure 34 shows the original transect of the bottom sensor in blue and the HT results in red. As desired the HT removed the dipole behavior creating a positive monopole. Figure 35 shows the original transect of the EMI conductivity in blue and the HT results in red. Once again the HT was effective at creating a positive monopole.

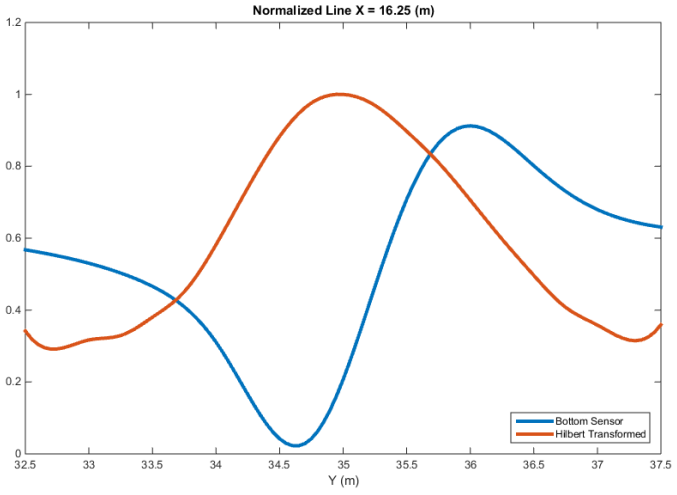

Figure 34 - MAG Transect and HT Mag Transect

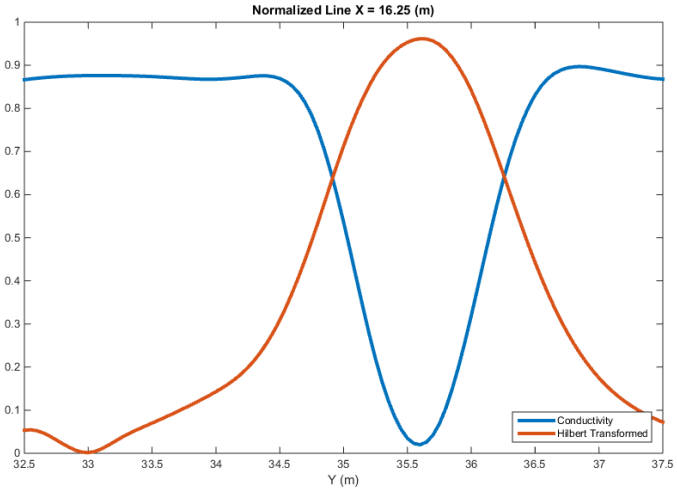

Figure 35 - EMI Transect and HT EMI Transect

In figure 36, the HT results of the MAG and EMI transects are shown. As desired both anomalies have been converted to positive monopoles, and are both qualitatively and quantitatively seen to be in similar locations. These same results can also be seen while looking at the entire sub-grid. Figure 37 shows EMI over MAG which once again can be recognized qualitatively to be in a similar location. Figure 38 shows the HT results which can quantitatively be shown in a similar location.

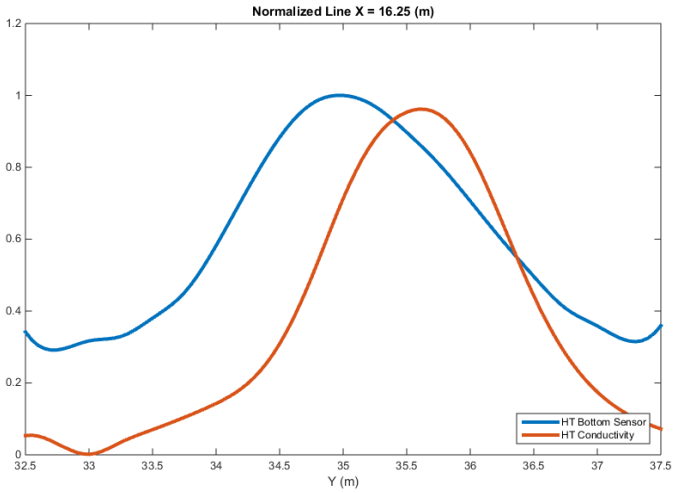

Figure 36 - HT MAG and HT EMI Transects in Sub-grid B

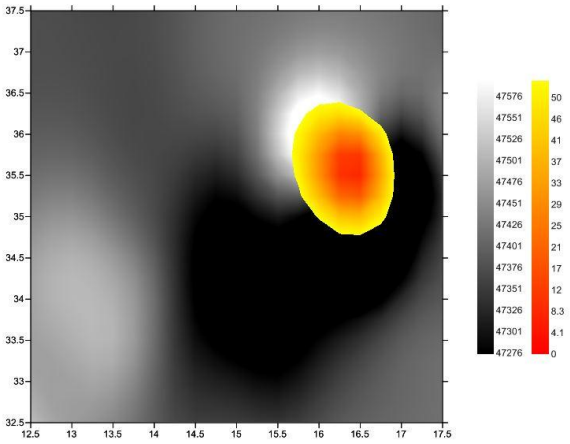

Figure 37 - EMI over MAG Sub-grid B

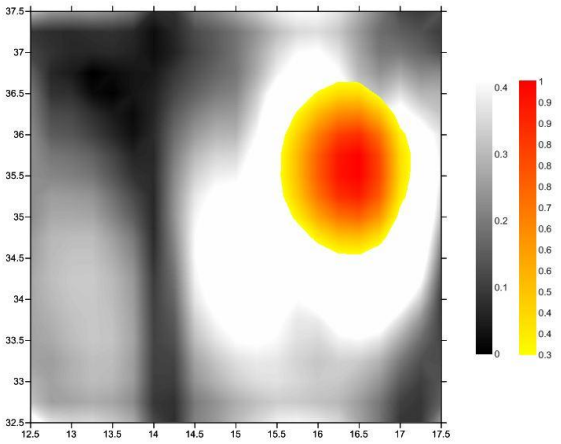

Figure 38 - HT EMI over HT MAG Sub-grid B

Figure 39 shows the full-grid HT MAG data. The data has been normalized on a 0 to 1 scale so that it can be compared to EMI. The HT MAG no loger consists of dipoles, only positive monopoles. Figure 40 shows the full-grid HT EMI data which has also been normalized on a 0 to 1 scale. The HT was succesfull at converting negative monopoles into positive monopoles.

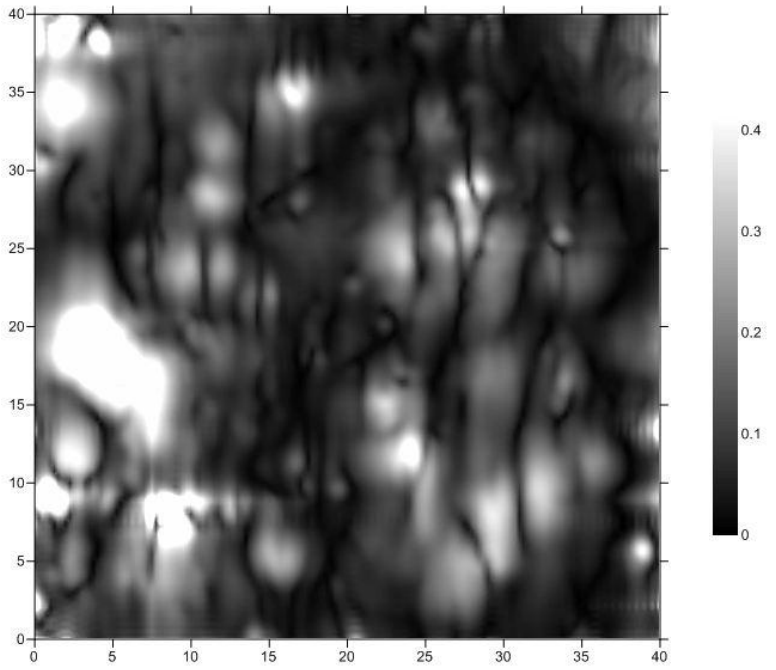

Figure 39 – Normalized HT MAG over full field

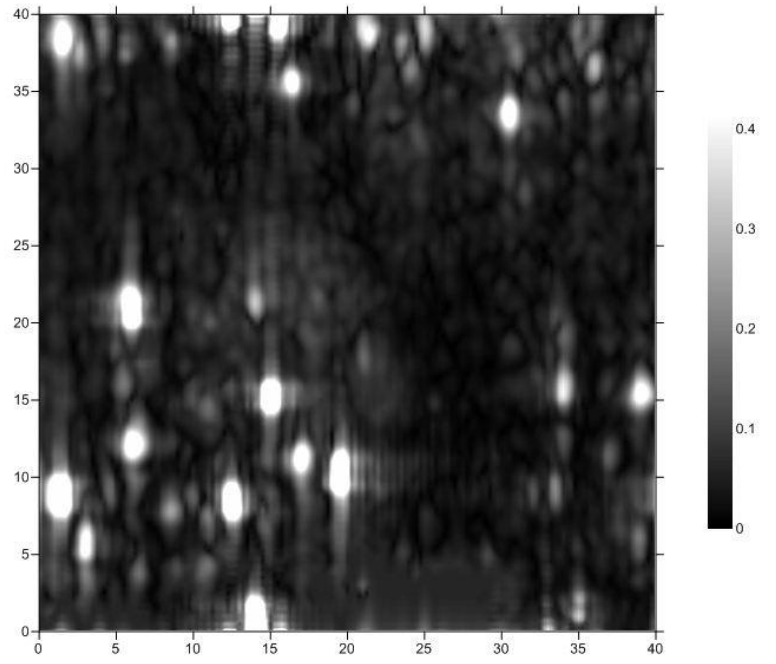

Figure 40 - Normalized HT EMI over Full Grid

CHAPTER IV

ANALYSIS

Analyzing all three geophysical techniques together provides a much clearer picture of the sub-surface than if the three techniques were analyzed separately. To achieve the best results, MAG, EMI, and GPR were both qualitatively and quantitatively analyzed.

Qualitative

Qualitative analysis was accomplished by anomaly overlay analysis, where the results of one method are depicted over the results of another method. Overlay analysis allows subjective visual correlation of different geophysical methods. Figure 41 depicts EMI anomalies in yellow over the background MAG bottom sensor in gray. There were several EMI anomalies that visually correlated with MAG anomalies, especially in the lower left area of the survey. This was expected as MAG detects anomalies from objects containing Iron (Fe) oxides and EMI can detect anomalies from all metals that produce secondary magnetic fields. Interestingly there was a large area where MAG anomalies were not detected by EMI anomalies.

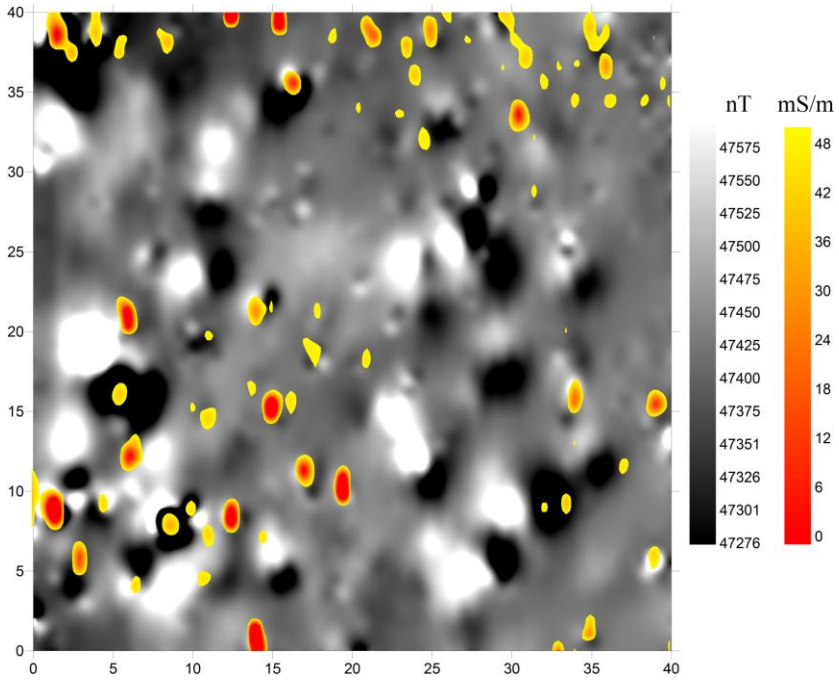

Figure 41 - EMI Conductivity over MAG Bottom Sensor

Figure 42 shows GPR depth slice from 5-10 cm in red over MAG bottom sensor in gray. In sub-grid B, in the upper portion of the survey, the GPR anomaly correlates very well with the MAG anomaly. In sub-grid A, several GPR anomalies have corresponding MAG anomalies, but the main structure seen in GPR is not seen in MAG, indicating that the structure is not magnetic. Figure 43 shows GPR depth slice from 5-10 cm in red over EMI conductivity in gray. Once again, the anomaly in sub-grid B is seen in both GPR and EMI. In sub-grid A, GPR anomalies correspond much better to EMI anomalies than MAG did. This can be attributed to EMI's ability to detect a wider array of objects than MAG. The main GPR structure is also seen in EMI as a general decrease in conductivity in the same area.

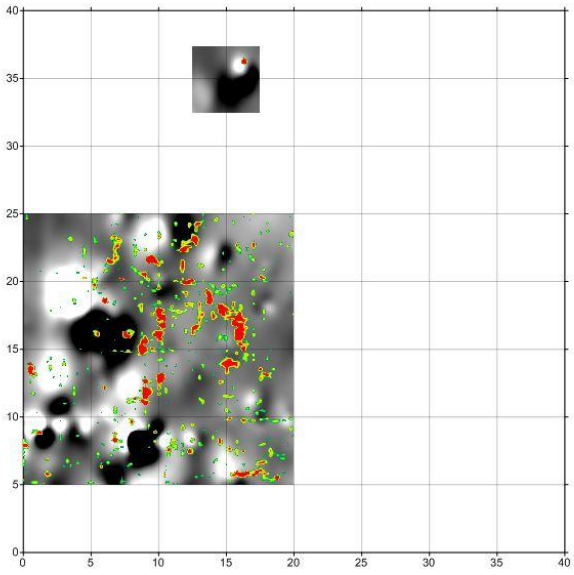

Figure 42 - GPR 5-10 cm over MAG Bottom Sensor

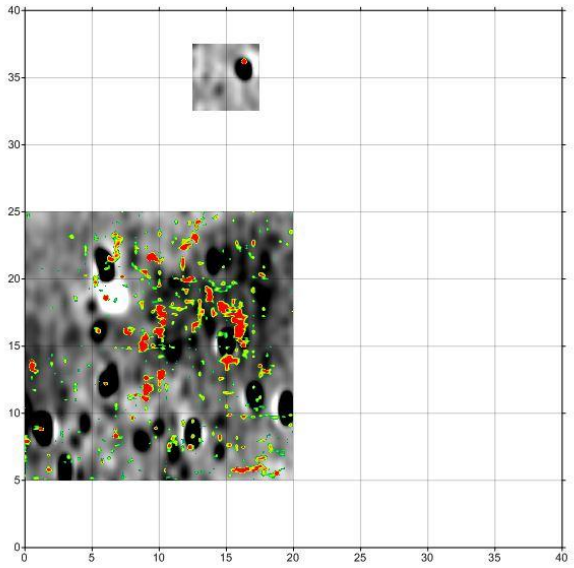

Figure 43 - GPR 5-10 cm over EMI Conductivity

Quantitative

To quantitatively analyze the data, magnitude thresholds were set to determine where anomalies are located. For a certain location to have correlated between different methods, it had to meet multiple threshold requirements. For example, if a data point met the requirements for a MAG

anomaly but not an EMI anomaly the point would be represented as only a MAG anomaly. If the data point met the requirements for both MAG and EMI anomalies the point would represent a correlated MAG and EMI anomaly. Figure 44 shows the full grid results of magnitude thresholding for MAG and EMI. No anomaly is shown in grey, MAG only anomalies in blue, EMI only anomalies in yellow, and correlated MAG and EMI anomalies in red. A similar result to the qualitative analysis between MAG and EMI is seen. There are several locations where MAG and EMI anomalies correlate very well, but again the right side of the grid sees MAG anomalies not associated with EMI anomalies.

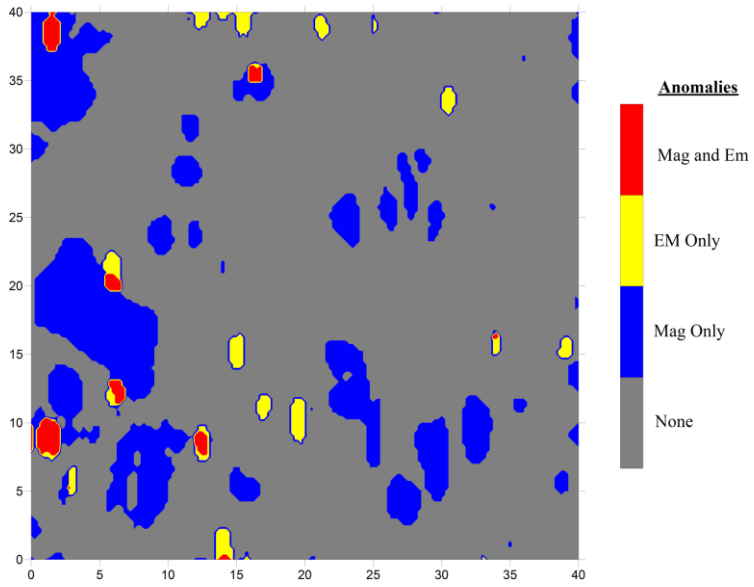

Figure 44 - Anomaly Thresholding of MAG and EMI data

Figure 45 shows sub-grid A results of magnitude thresholding on GPR and EMI data. GPR anomalies are shown in blue, EMI anomalies in yellow, and correlated anomalies in red. Almost all EMI anomalies have a corresponding GPR anomaly. However, there are GPR anomalies that do not correlate to EMI anomalies.

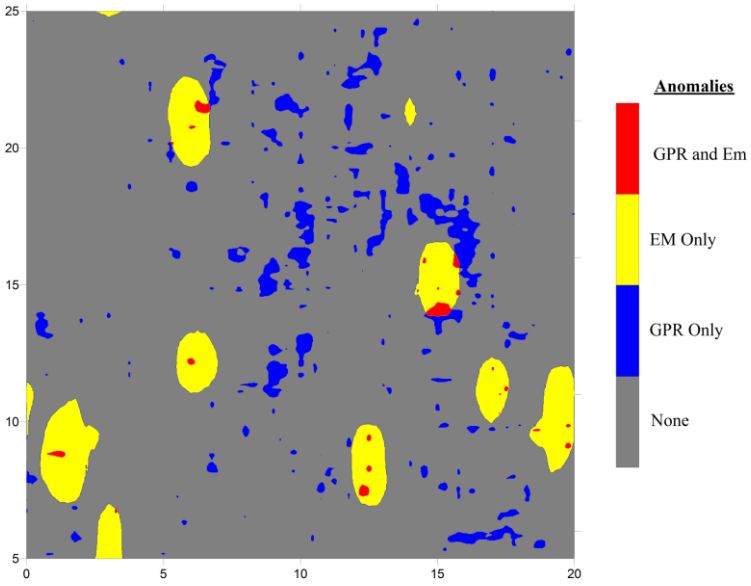

Figure 45 - Anomaly Thresholding of GPR and EMI

CHAPTER V

CONCLUSIONS

Ultimately the project objectives were met. An unknown sub-surface structure was located using a variety of geophysical methods, and student accessibility to geophysical equipment and software was increased.

Mag Cart and GeopMapper

Both Mag Cart and GeopMapper were successful in their intended roles. Mag Cart allowed magnetometer sensors to keep a constant ground clearance height throughout the MAG survey, while also allowing for increased data collection speed. The design of the Mag Cart will be improved by using larger wheels to reduce bouncing in rough terrain and by using a non-magnetic aluminum construction to increase rigidity of the cart. GeopMapper was able to process both MAG and EMI data effectively, while maintaining a short learning curve for students. In the future, GeopMapper will be improved by adding additional filters, and an improved user interface.

Hilbert Transform

The Hilbert Transform was used on MAG and EMI data to change the nature of anomalies in the data. While the Hilbert Transform was effective at this, there were also some unintended consequences. The 2-D Hilbert Transform produced a crosshair pattern on large anomalies. This is not ideal and will be improved in future work. The Hilbert Transform also suppressed smaller

anomalies. Even though larger anomalies were preserved, subtle features in the data can be beneficial and should not be overlooked when using the Hilbert Transform.

Qualitative vs. Quantitative Analysis

In order to visualize data from multiple geophysical methods, both qualitative and quantitative analysis were used. To quantitatively analyze the data, magnitude thresholding was used to locate anomalies. While this was effective, there was a certain loss of information associated with the process. In the future, other methods of quantitative analysis should be examined. Qualitative overlay analysis was extremely effective at visualizing different geophysical methods. Both large and small anomalies were preserved and visualized. Ideally both methods of analysis should be used to completely understand the data. Overlay analysis has the ability to stand alone as an analysis technique, while magnitude thresholding does not.

Historical Significance

The Historical significance of the site has yet to be determined. However, three geophysical methods each revealed substantial anomalies in the subsurface. Some of these anomalies were consistent throughout multiple techniques. In order to prove the existence of structures in the sub-surface, Archeological excavation of the site is recommended. The data from the three geophysical methods indicates that the survey should focus on the areas in sub-grids A and B. Once the archeological survey is completed, final conclusions about the site will be made.

REFERENCES

Brass, S., 2011, The burning of Brenham: Brenham, TX, Main Street Brenham, 72 p.

Everett, M., 2013, Near-Surface Applied Geophysics: New York, Cambridge University Press.

Hasskarl, R., 1933, A History of Brenham, Brenham, Texas, Mrs. Robert Hasskarl.

MagMap2000 (Version 4.98) [Software], (2000), California: Geometrics, Retrieved from, http://www.geometrics.com/geometrics-products/geometrics-magnetometers/download-magnetometer-software/.

Meehan, T., 2014, Multisensor Geophysical Fusion For Improved Sub-Surface Imaging at Historic Camptown Cemetery, Brenham, TX [B.S. of Geophysics Undergraduate]: Texas A&M University.

Taner, M. T., Koehler, F., and Sherrif, R. E., 1979, Complex seismic trace analysis, Geophysics, v. 44, pp 1041-1063.

W. C. A. District, 2014, Property Detail sheet (R42537), Volume 2014: Washington County, Washington County Appraisal District. http://www.washingtoncad.org/Appraisal/PublicAccess/

Young, C. T., 2004, Basic Magnetic Processing and Display in MATLAB